J|A|C|S ARTICLES

Published on Web 03/31/2010

What the Cell "Sees" in Bionanoscience

Dorota Walczyk,[†,‡] Francesca Baldelli Bombelli,*[,†,‡] Marco P. Monopoli,[†,‡] Iseult Lynch,[†,‡] and Kenneth A. Dawson*[,†,‡]

Centre for BioNano Interactions, School of Chemistry and Chemical Biology, and UCD Conway Institute for Biomolecular and Biomedical Research, University College Dublin, Belfield, Dublin 4, Ireland

Received December 18, 2009; E-mail: Kenneth@fiachra.ucd.ie; Francesca.baldelli@fiachra.ucd.ie

Abstract: What the biological cell, organ, or barrier actually "sees" when interacting with a nanoparticle dispersed in a biological medium likely matters more than the bare material properties of the particle itself. Typically the bare surface of the particle is covered by several biomolecules, including a select group of proteins drawn from the biological medium. Here, we apply several different methodologies, in a time-resolved manner, to follow the lifetime of such biomolecular "coronas" both *in situ* and isolated from the excess plasma. We find that such particle−biomolecule complexes can be physically isolated from the surrounding medium and studied in some detail, without altering their structure. For several nanomaterial types, we find that blood plasma-derived coronas are sufficiently long-lived that they, rather than the nanomaterial surface, are likely to be what the cell sees. From fundamental science to regulatory safety, current efforts to classify the biological impacts of nanomaterials (currently according to bare material type and bare surface properties) may be assisted by the methodology and understanding reported here.

Introduction

Nanoparticles (NPs) interact with cells (and living organisms in general) in a fundamentally different manner than do small molecules. The latter, broadly speaking, diffuse into and around the cell, partitioning freely according to near-equilibrium principles. In contrast, nanoparticles, because of their size, are processed and taken into the cell by active, energy-dependent processes. In such active processes, the primary contact between nanoparticles and living organisms is mediated via the "nanoparticle" surface in the biological medium.[1−7] Perhaps surprisingly, given the high level of interest in bionano interactions with living organisms, relatively little has been reported about the structure and organization of the nanoscale objects in the biological media in which they are studied.[8−14] This is in striking contrast to the deep and mature knowledge of physiochemical properties of these systems in simple solvents.

We begin by noting that "spontaneous accumulation of proteins at the solid-water interface, which alter the characteristics of the sorbent surface, can form quite durable coatings",[15] and this has even been used in seeking to understand the acute biological responses to medical devices. For nanoparticulates however, it is surprising that when limited numbers and types of biomolecules compete for the curved nanoparticle surface, the resulting biomolecule "corona" contains only a few (mostly identifiable) proteins, in many cases differing from those adsorbed to flat surfaces of the same material.[7,9,13,16−19] What the cell actually "sees" during (for example) the nanoparticle uptake into the cell, or other biological processes, requires us to know if those bound proteins stay there for long enough to

[†] Centre for BioNano Interactions.
[‡] UCD Conway Institute for Biomolecular and Biomedical Research.

(1) Watson, P.; Jones, A. T.; Stephens, D. J. *Adv. Drug Delivery Rev.* **2005**, *57*, 43–61.
(2) Jiang, W.; KimBetty, Y. S.; Rutka, J. T.; ChanWarren, C. W. *Nat. Nanotechnol.* **2008**, *3*, 145–150.
(3) Rejman, J.; Oberle, V.; Zuhorn, I. S.; Hoekstra, D. *Biochem. J.* **2004**, *377*, 159–169.
(4) Gratton, S. E. A.; Ropp, P. A.; Pohlhaus, P. D.; Luft, J. C.; Madden, V. J.; Napier, M. E.; DeSimone, J. M. *Proc. Natl. Acad. Sci. U. S. A.* **2008**, *105*, 11613–11618.
(5) Chithrani, B. D.; Chan, W. C. W. *Nano Lett.* **2007**, *7*, 1542.
(6) Mahmoudi, M.; Simchi, A.; Imani, M. *J. Phys. Chem. C* **2009**, *113*, 9573–9580.
(7) Ehrenberg, M. S.; Friedman, A. E.; Finkelstein, J. N.; Oberdorster, G.; McGrath, J. L. *Biomaterials* **2009**, *30*, 603–610.
(8) Cedervall, T.; Lynch, I.; Foy, M.; Berggård, T.; Donnelly, S. C.; Cagney, G.; Linse, S.; Dawson, K. A. *Angew. Chem.* **2007**, *46*, 5754–5756.
(9) Cedervall, T.; Lynch, I.; Lindman, S.; Nilsson, H.; Thulin, E.; Linse, S.; Dawson, K. A. *Proc. Natl. Acad. Sci. U. S. A.* **2007**, *104*, 2050–2055.
(10) Chanteau, B.; Fresnais, J.; Berret, J.-F. *Langmuir* **2009**, *25*, 9064–9070.
(11) Göppert, T. M.; Müller, R. H. *Int. J. Pharmacol.* **2005**, *302*, 172–186.
(12) Lindman, S.; Lynch, I.; Thulin, E.; Nilsson, H.; Dawson, K. A.; Linse, S. *Nano Lett.* **2007**, *7*, 914–920.
(13) Lundqvist, M.; Stigler, J.; Cedervall, T.; Elia, G.; Lynch, I.; Dawson, K. *Proc. Natl. Acad. Sci. U. S. A.* **2008**, *105*, 14265–14270.
(14) Nel, A.; Madler, L.; Veregol, D.; Xia, T.; Hoek, E. M. V.; Somasundaran, P.; Klaessig, F.; Castranova, V.; Thompson, M. *Nat. Mater.* **2009**, *8*, 543–557.
(15) *Physical Chemistry of Biological-Interfaces*; Marcel Dekker: New York, 1999.
(16) Lynch, I.; Dawson, K. A. *Nanotoday* **2008**, *3*, 40–47.
(17) Simberg, D.; Park, J.-H.; Karmali, P. P.; Zhang, W.-M.; Merkulov, S.; McCrae, K.; Bhatia, S. N.; Sailor, M.; E., R. *Biomaterials* **2009**, *30*, 3926–3933.
(18) Mu, Q.; Li, Z.; Li, X.; Mishra, S. R.; Zhang, I. B.; Si, Z.; Yang, L.; Jiang, W.; Yan, B. *J. Phys. Chem. C* **2009**, *113*, 5390–5395.
(19) Hellstrand, E.; Lynch, I.; Andersson, A.; Drakenberg, T.; Dahlback, B.; Dawson, K. A.; Linse, S.; Cedervall, T. *FEBS* **2009**, *276*, 3372–3381.

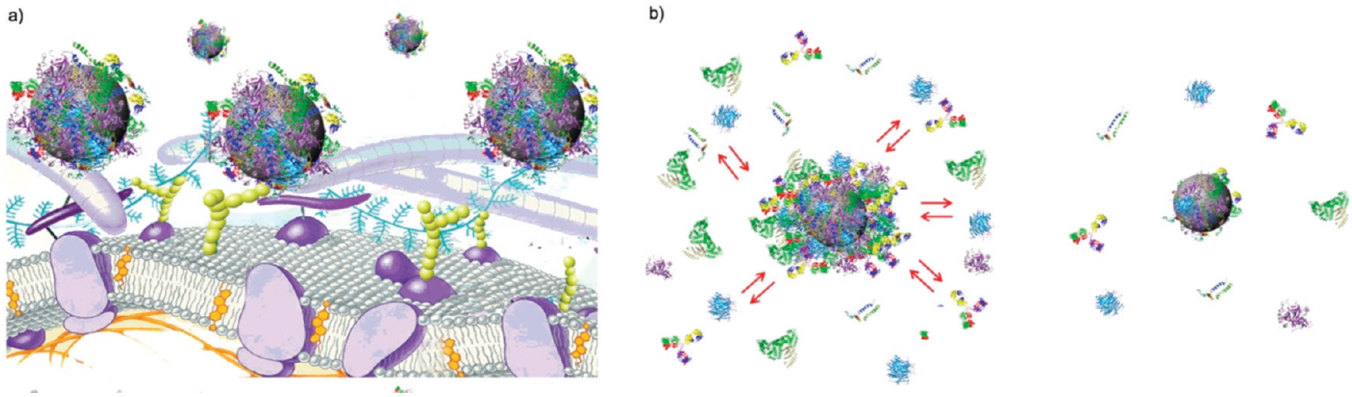

Figure 1. (a) Cartoon representation of the possible exchange/interaction scenarios at the bionanointerface at the cellular level. (b) Schematic drawing of the structure of NP−protein complexes in plasma: the "core" nanoparticle is surrounded by the protein corona composed of an outer weakly interacting layer of protein (left, full red arrows) rapidly exchanging with a collection of free proteins and a "hard" slowly exchanging corona of proteins (right). Diagram is not to scale in representing the proportions of the different objects.

be biologically significant. For those with sufficiently slow exchange kinetics, the corona itself constitutes the primary contact to the cells.[8,9] Within the present paper we now establish conclusively that the typical biomolecular residence time on nanoparticles implies that the particle-bound proteins will be the primary biologically relevant species.

Relevant kinetic processes to consider include exchange of proteins between the nanoparticle surface and the plasma, the NP surface and the cell surface (including any specific receptors of interest), and high-affinity free protein molecules in the medium that could compete for the cell surface, as shown schematically in Figure 1a. We hypothesize that the cell "sees" a system in which the core nanoparticle (and other multiparticle assemblies) is surrounded by a "hard" corona of slowly exchanging proteins and an outer (weakly interacting, and rapidly exchanging) collection of proteins (Figure 1b).[20] Other forms of multimeric particle−protein complexes may also be present, depending on the dispersion. Collectively these particle−protein complexes constitute "what the cell sees".

If the slowly exchanging proteins have sufficiently long residence times, then *de facto* the effective unit of bionanoscience is a nanoparticulate core and an associated biomolecule corona that is so strongly bound that the particle itself is merely the scaffold for the proteins. We emphasize that our interest is to understand these questions for complex biological media (such as plasma, tissue culture serum, and organ-derived fluids). For model systems, involving single proteins, interesting and elegant studies already exist.[21−25]

In this article we show that several common nanoparticles dispersed in blood plasma lead to extremely long-lived coronas, as well as new types of organized protein−particle assemblies (multimeric protein−particle complexes). Our previous studies have focused on the identity of the bound proteins using proteomics. Now, by applying a combination of techniques such as differential centrifugal sedimentation (DCS), dynamic light scattering (DLS), and transmission electron microscopy (TEM) we develop a basic structural picture of nanoparticles in biological media and establish a platform for future studies of "what the cell sees". Such studies will also enable much more advanced proteomics tools to be applied and mapping of the conformation of the outer layers (epitopes) actually in contact with the cellular machinery.

Results

We present results for dispersions of surface-carboxylated polystyrene particles (PSCOOH) and surface-sulfonated polystyrene nanoparticles ($PSOSO_3H$) both of nominal sizes 100 and 200 nm, as well as for silica particles (SiO_2) of nominal size 50 nm, all incubated in human blood plasma. These particular nanoparticles are of very great interest, being part of the first group of materials to be evaluated for safety at the nanoscale.[26] However, from our point of view their role is as "standard nanoparticles" addressing several different representative issues of surface and size, allowing us to extract a general idea about their corona structure and organization in biological media. Basic physicochemical characteristics of all bare particles are given in Tables S1a and S1b in the Supporting Information (SI).

Particles are studied by DCS under several different conditions including in full (diluted in PBS) plasma and also after having been spun down and resuspended in PBS buffer before and after centrifugation and washing off of the excess (unbound or loosely bound) proteins (see Materials section in the SI for full details of the sample preparation). This permits a connection to be made between the particle−corona complexes in isolation and the complexes *in situ* in the presence of excess plasma.

Full details of the DCS approach are given in the Methods section in the SI, but we remark that it can be made remarkably reproducible, with striking precision (we show DCS results for particle size distribution in several independent experiments in Figure S1 in the SI). The method is one of very few techniques that can be applied to complex biological systems, without the need for fluorescent labels and other such devices, or for extreme nanoparticle dilution. Essentially all variations in our experiments derive from the nature of complex biocolloidal and

(20) Lynch, I.; Cedervall, T.; Lundqvist, M.; Cabaleiro-Lago, C.; Linse, S.; Dawson, K. A. *Adv. Colloid Interface Sci.* **2007**, *167*, 134–135.
(21) Röcker, C.; Pötzl, M.; Zhang, F.; Parak, W. J.; Nienhaus, G. U. *Nat. Nanotechnol.* **2009**, *4*, 577–580.
(22) Rezwan, K.; Studart, A. R.; Vörös, J.; Gauckler, L. J. *J. Phys. Chem. B* **2005**, *109*, 14469–14479.
(23) Xiao, Q.; Zhou, B.; Huang, S.; Fangfang, T.; Guan, H.; Ge, Y.; Liu, X.; He, Z.; Liu, Y. *Nanotechnology* **2009**, *20*, 325101.
(24) Aubin-Tam, M.-E.; Hamad-Schifferli, K. *Biomed. Mater.* **2008**, *3*, 034001.
(25) Vauthiera, C.; Lindnerc, P.; Cabaned, B. *Colloids Surf., B* **2009**, *69*, 207–215.
(26) http://www.olis.oecd.org/olis/2008doc.nsf/LinkTo/NT00003282/$FILE/JT03246895.PDF.

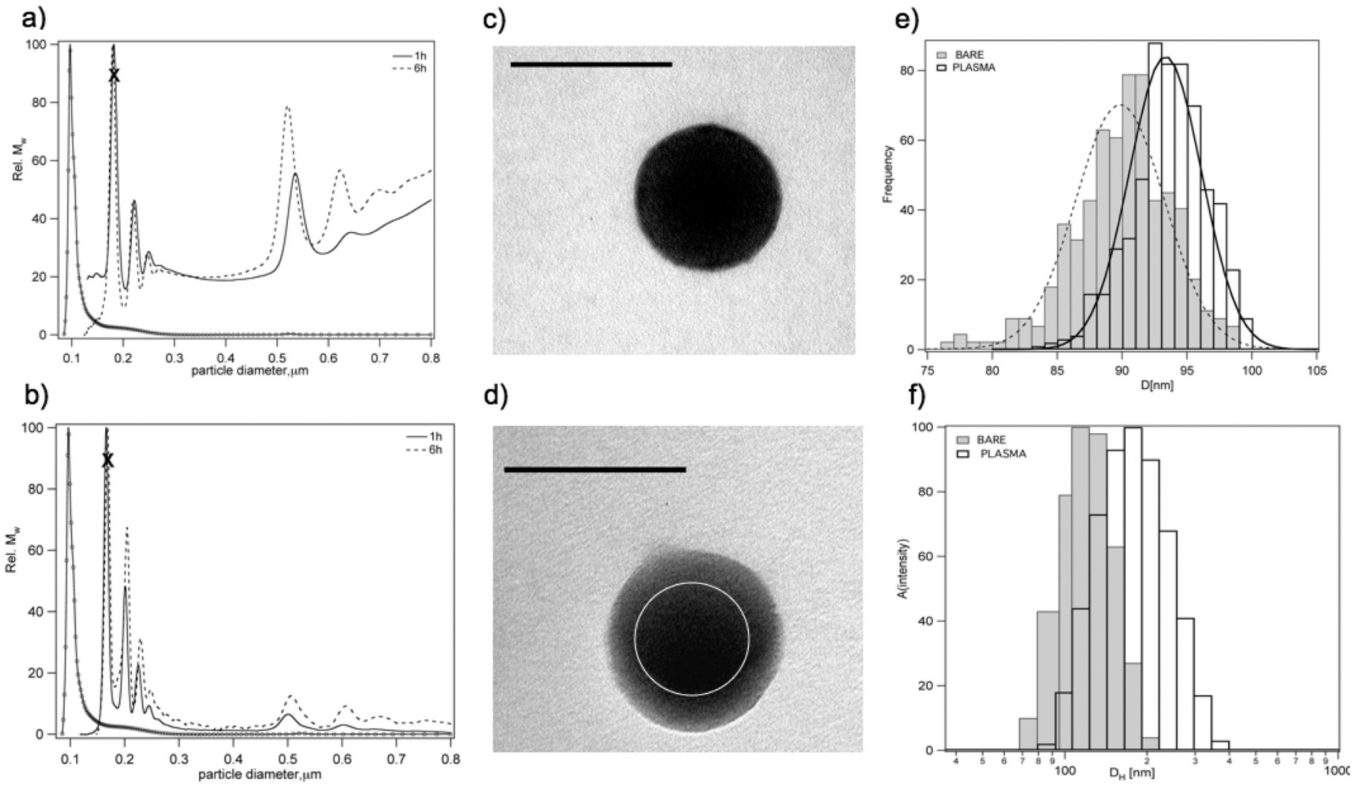

Figure 2. (a) DCS results for 100 nm PSCOOH NP−protein complexes *in situ* (full plasma) measured after 1 h (full line) and 6 h (dotted line) of incubation. (b) DCS results for particle−corona complexes free from excess plasma (washed) measured 1 and 6 h after the redispersion in PBS. Bare 100 nm PSCOOH NPs in PBS (open circles) are reported for reference in both graphs. The marked peaks relate to the monomeric NP−protein complexes. (c) TEM picture of bare 100 nm PSCOOH nanoparticles fixed in 2.5% gluteraldehyde solution. Bar = 100 nm. (d) TEM picture of the protein−particle complex (free from excess plasma) for 100 nm PSCOOH NPs fixed in 2.5% glutaraldehyde solution. The white circle is drawn as a guide to the eye; other images are reported in Figure S3c in the SI. Bar = 100 nm. (e) Size distribution histogram obtained by size analysis of several TEM images of particles (about 500 NPs were evaluated), in order to obtain meaningful statistical results for the particle size. (f) DLS intensity-weighted size distribution obtained by CONTIN for 100 nm PSCOOH NPs (bare) and 100 nm PSCOOH protein−particle complexes free from excess plasma (washed corona) in PBS.

nanoparticle systems. In comparison to those, one may ignore all errors on the relevant time and length scales due to DCS, including those arising from use of independent samples for time-resolved experiments. We also note that, though explicit complex sizes can be deduced, the main scientific issues regarding the corona behavior are settled by the temporal stability of the complexes, rather than detailed size information. Therefore, we do not emphasize efforts to rationalize absolute sizes between quite different methods that measure slightly different quantities, but instead focus on the difference in size between bare and corona-coated systems. For example, to identify a true size from DCS, one must know the shape and internal density distribution of each aggregate, so instead we present the data in an unbiased but physically realistic format of (on the *x*-axis) the equivalent diameters for spheres of homogeneous density and (on the *y*-axis) relative "apparent" molecular weight. For monomeric nanoparticle−protein complexes we compute the "true" size of the nanoparticle−protein complex and the corona size using a simple core−shell model of two densities (bare particle material density and adsorbed protein-biomolecule density). Details are given in the Methods section in the SI (Tables S2a,b).

In Figure 2a we introduce the basic DCS data for PSCOOH 100 nm NPs (*in situ*) in full plasma (diluted 50 times with PBS) after one hour and six hours of incubation. All peaks and the small changes that occur in them during this time period are reproducible, and we find that, for many materials, the protein corona is formed in a relatively stable manner over a period of one hour, although much slower and more subtle changes continue for as long as 12 hours. In Figure 2b we show data from the particle−corona complexes isolated by spinning down the mixture studied in Figure 2a, washing to remove residual proteins, and resuspending in PBS (data for spun down, but unwashed particle−protein complexes are given in Figure S3a) at the same nominal particle concentration as the sample in full plasma (Figure 2A). The measurements are carried out one hour and six hours after redispersion (i.e., isolation of the complexes, washing steps, and then redissolution in PBS followed by measurement after 1 or 6 h) for comparison with the *in situ* system. The similarity of the peaks for washed particles and particles (*in situ*) in plasma is truly striking.

Results are typical of many nanomaterials we have studied (including all but one of those reported here). Thus, we find a shifted nanoparticle monomer peak and several other populations that have typical incremental sizes consistent with rotationally averaged particle−corona dimers, trimers, and so forth. There is a larger peak (nominally at around half a micrometer in size) present in the experiments, including in plasma itself (see Figure S2a), but such protein clusters are far fewer in number than the monomeric nanoparticle complexes. In fact, the plasma peak at 500 nm is sensitive to the source of plasma (with varying peak intensity and position resulting from different donation sessions; see Methods section in the SI for details), and DCS experiments on pure plasma from different sources can give slightly different distributions of the aggregate species. In some cases the peak (normally at about 500 nm assuming PS particle

density) appears more as a weak background signal than a real peak. However, the DCS size distributions of the protein−particle complexes obtained from incubation of the NPs in all plasma samples are remarkably reproducible. For the sake of clarity, most data are from the same source of plasma (same donation session), whose DCS spectrum is reported in Figure S2a in the SI. For comparison a single example of particle−protein complexes from another plasma source (without a pronounced presence of aggregates) is given in Figure S5c. Identical experimental conditions have been used (sucrose gradient, disk angular velocity, etc.) in these experiments, so we can relate the pure plasma peaks (broad background peak at 200 nm and others near 500 nm in Figure S2a) to the background in the particle−plasma results. We conclude that when particles are added to the plasma (see Figure 2a), the nominal particle monomer peak shifts to larger size and the "plasma" peak is also shifted, but preserved in its general form.

This isolation of the particle−protein complexes by spinning and multiple washing steps (Figure 2b) indicates that the monomer−protein complex and large protein−particle associated complexes are retained with essentially the same sizes as they have *in situ* in plasma. Very small differences between the systems are possibly due to drag effects due to the complex plasma medium, and much smaller variations in washed sample sizes continue to evolve as a function of wash number. After three or four washes such variations become much smaller (see Figure S2b in the SI).

To give additional qualitative support for the broader conclusions and to confirm the stability of the isolated complexes, we present electron microscopy data for bare particles compared to particles with a hard protein corona in Figure 2c,d (see Methods section in the SI for details of the sample preparation). Such images need to be interpreted carefully, as the particles themselves are somewhat polydisperse in size, and sample preparation affects the protein conformation, so the corona thickness is hard to determine. Still, both these and other representative selections of images (Figure S3c,d in the SI) show clear evidence of a thin additional plasma-derived layer around the particles following incubation in plasma. These adsorbed layers completely coat the particles and also coat those particles involved in larger aggregates (see Figure S3d in the SI). A statistical analysis (Figure 2e) of the size of the NPs (based on about 500 NPs) results in a Guassian distribution for both bare and protein-coated NPs, with the average diameter being 5 nm larger for the coated NPs than the bare ones.

DLS experiments on the protein−particle complexes free from excess plasma (washed system) were also performed as a function of the scattering vector q. The results are typical of a monomodal distribution of particles, and the corresponding average hydrodynamic diameter is 180 nm, about 50 nm larger than the hydrodynamic diameter (D_H) of the bare nanoparticles. This value is in good agreement with previous DLS results for gold NPs incubated in plasma.[27] Since populations of other species (dimer, trimer, etc.) are not resolved in light scattering, appearing instead as a broadening of the apparent size (Figure 2f), this increase cannot be quantitatively related to the thickness of the protein layer. However, these results agree with the conclusion of a robust protein coating on the nanoparticles upon incubation in plasma.

The complexes are sufficiently stable and the DCS method is sufficiently reproducible to perform more explicit time-resolved studies of the protein−particle complex stability. Formally, the fluctuation dissipation theorem implies that the "corona off-rate" (from fluctuations that reduce the corona) could be determined using the fact that *in situ* off-rates should be the same as those obtained by near-equilibrium kinetics after minimal plasma dilution. Evidently, when ambient plasma is removed and the particles are redispersed in PBS, the chemical potential of the adsorbed proteins will be much lowered in the dispersing medium (PBS), and there will be a strong thermodynamic force for those proteins to detach from the particle. The time taken for this process to occur is a lower boundary to the biomolecular "off-rate" *in situ* in plasma. In practice we find the corona to be so stable that the detailed kinetics are not so important. We simply place the washed and unwashed corona samples into PBS and follow the time evolution of the complex.

We next show the overall population evolution of particle−protein complexes for washed (Figure 3a,b) and unwashed (Figure 3c,d) samples of surface-carboxylated particles as a function of time following redispersion in PBS. The hard corona−monomer complex (washed) is almost unchanged over the time period, although there is some evidence of modest multimeric rearrangements. In the case of the unwashed sample, where there are some excess proteins present, these continue to be added to the corona. This may suggest that the "free" residual proteins after spinning (but not washing) have a higher affinity for the particles than typical for the proteins in plasma. We have also studied the time evolution of the protein−corona complexes following redispersion in PBS by DLS at large angle ($\theta = 173°$) in order to minimize the cluster and aggregate contributions. The results are reported in Table 1, and the general trend is in good agreement with that seen with DCS. Again, in the washed system size is almost unchanged with time (following redispersion) and the size distribution remains centered on the same value with minor changes in the width, as shown by the $\langle D_H \rangle$ values, while for the unwashed system an increase of the apparent hydrodynamic size is observed with time, consistent with the increased affinity of the proteins for the particle surface mentioned above.

We reiterate that the data from DCS are presented as effective sizes assuming a sphere of uniform density that is the same as the core nanomaterial. For monomer−protein complexes a more accurate size (and thereby thickness of the protein shell) may be calculated by assuming a core−shell model as explained in the Methods section and as shown in Tables S2a,b in the SI. For the hard-corona monomer complexes of 100 nm PSCOOH NPs the shell thickness value, roughly 10 nm, is consistent with the size extracted from the TEM images (see Figure 2c−e and Figure S3c,d in the SI) and with those calculated by DLS (given that the latter refers to hydrodynamic sizes and includes multimer averaging).

While not seeking to reiterate previous work on the composition of the corona, it is worth establishing clearly that the increment in size shown by DCS is associated with specific proteins. Therefore in Figure S4 we show how the composition of the hard corona of the 100 nm PSCOOH NPs (related to Figure 3a,b) evolves over time. A time-resolved extraction (by the usual procedure used to unbind the corona) is presented, which shows that both the protein pattern and the intensities of the different bands are consistent over time[7,8] (see ref 13 for the details of the experimental procedure and the identity of the proteins in the bands). The fact that the structure and

(27) Dobrovolskaia, M. A.; Patri, A. K.; Zheng, J.; Clogston, J. D.; Ayub, N.; Aggarwal, P.; Neun, B. W.; Hall, J. B.; McNeil, S. E. *Nanomedicine* **2009**, *5*, 106–117.

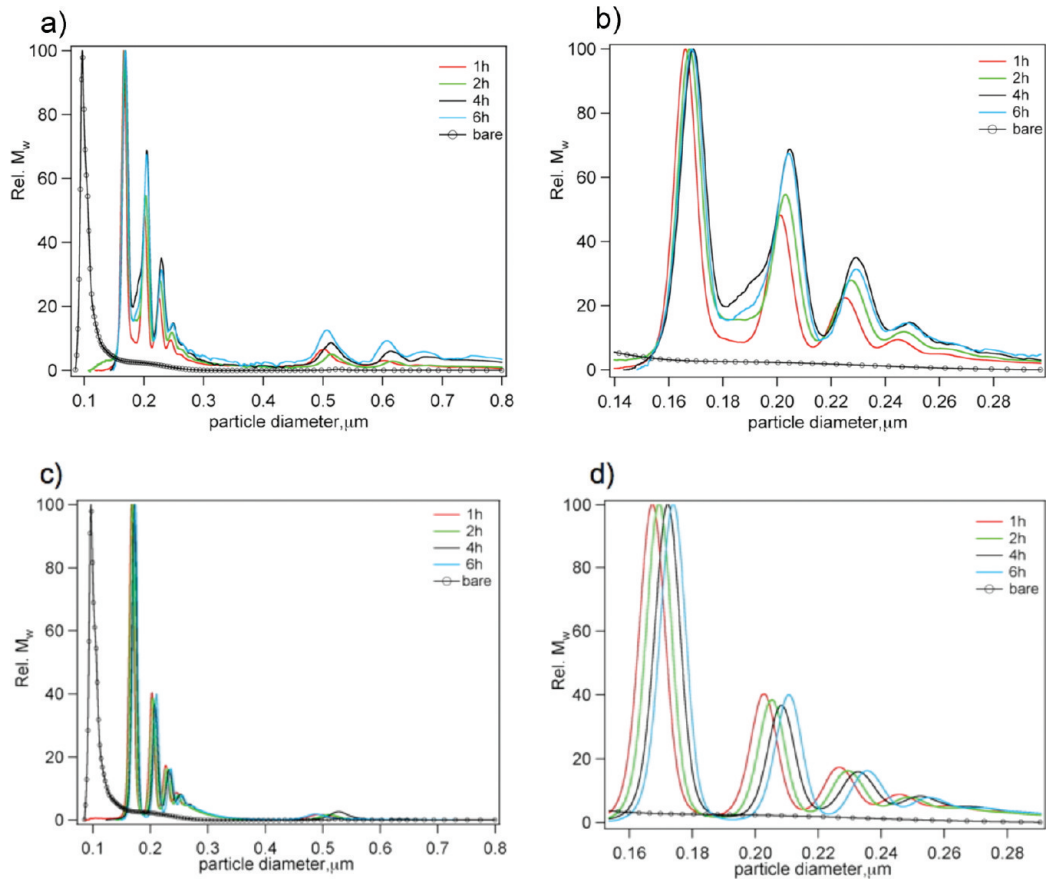

Figure 3. (a) DCS data for 100 nm PSCOOH NP−protein complexes free from excess plasma (washed system) as a function of time. (b) Enlargement of the monomeric particle−protein peak together with the dimer and trimer peaks. (c) NP−protein complexes (unwashed) free from excess plasma and resuspended in PBS without washing. The sample was measured as a function of time. The legend is reported in the inset. (d) Enlargement of the main peak areas of the DCS graph reported in Figure 3c to enhance the shift to larger size with time. The legend is reported in the inset. Bare PSCOOH NPs in PBS (open circles) are reported for reference.

Table 1. Time-Resolved DLS and Zeta-Potential Data for 100 nm PSCOOH NP−Protein Complexes at 25 °C and $\theta = 173°$

PSCOOH NPs	time [h]	D_H[a] [nm]	PDI[b]	$\langle D_H \rangle$[c] [nm]	z-potential [mV]
washed (1:50)	0	156.6 ± 3.9	0.071	170.4 ± 3.1	−8.8 ± 0.8
washed (1:50)	1	158.9 ± 4.5	0.060	172.1 ± 3.0	−8.0 ± 0.9
washed (1:50)	4	151.4 ± 3.5	0.043	162.4 ± 3.0	−9.8 ± 0.6
washed (1:50)	6	155.1 ± 3.5	0.050	167.0 ± 3.2	−8.9 ± 0.5
unwashed (1:50)	0	167.1 ± 6.4	0.096	185.1 ± 5.6	−7.8 ± 1.0
unwashed (1:50)	1	166.8 ± 2.8	0.078	183.1 ± 2.5	−7.5 ± 0.1
unwashed (1:50)	4	177.1 ± 3.0	0.094	198.9 ± 5.1	−9.2 ± 0.8
unwashed (1:50)	6	177.5 ± 3.0	0.095	198.3 ± 4.5	−9.2 ± 0.5

[a] z-average hydrodynamic diameter extracted by cumulant analysis of the data. [b] Polydispersity index from cumulant fitting. [c] Average hydrodynamic diameter determined from CONTIN size distribution.

composition of the hard corona remains relatively unchanged over time is thereby confirmed.

In Figure S5a−c and Table S3 we reproduce the same experimental data for the case where the NP−protein complexes, once separated from excess plasma, are redispersed in PBS at much higher dilution (1:500). This might be considered an extreme case (in which the chemical potential for corona detachment is changed greatly) for comparison and not one likely to be relevant to a biological or an *in vivo* context. For the *in situ* and carefully washed samples we see little change (over 6 h following redispersion) in the size distribution of the protein−particle complexes (see Figure S5a,c in the SI), consistent with the observations for the more concentrated sample. For the unwashed sample (S5b in the SI) there is a less pronounced tendency of the proteins to reassociate to the corona than was the case at 1:50 dilution, possibly due to the higher dilution.

A summary of the time-dependent changes in the thickness of the protein corona of the monomeric protein−NP complexes diluted 50 times in PBS is given in Figure 4 (and an analogous summary for 1:500 dilution is shown in Figure S5d in the SI), where the monomeric particle−protein complex size is shown in terms of the shell (corona) thickness determined by DCS data. In detail, there are several variations of interest. Clearly the number of washes (up until four) leads to different amounts of residual proteins that can associate in different ways when the sample is resuspended for study. However, after sufficient washes, the size of the corona after resuspension is unchanged over many (we show six) hours. Thus, the broad conclusion is that the adsorbed protein layer is remarkably stable over time for both dilutions (1:50 and 1:500), consistent with all data shown in this paper.

These same sorts of experiments have also been carried out with surface-carboxylated particles (PSCOOH) of 200 nm, and the results are reported in Figure S6a−g in the SI. We do not discuss them in detail since the broad outcomes are essentially similar to those reported for the 100 nm PSCOOH particles. Interestingly, the original 200 nm bare particles also exhibit signatures of bare particle dimers and trimers (for example, the dimers have precisely the size expected in DCS). This allows for comparison with the washed particle−protein complex

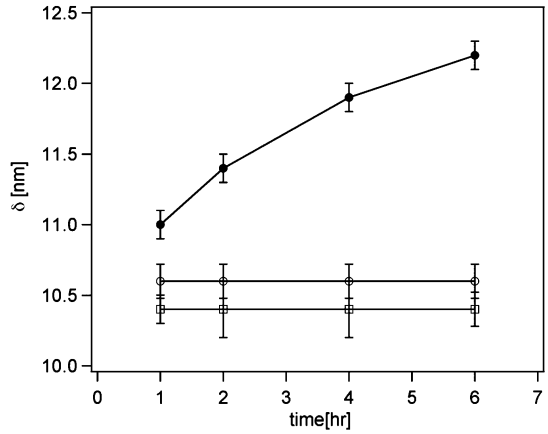

Figure 4. Protein shell thickness, calculated from the size of the main peak of the DCS data according to eq 6 in the Methods section of the SI, for 100 nm PSCOOH NP−protein complexes free from excess plasma [(●) unwashed, (○) sample subjected to two washings, (□) sample subjected to four washings] diluted 50 times in PBS (relating to Figure 3a,c). The error bars are expressed as the standard deviation of three measurements.

sample, and there we see clearly the particle dimers again, but with the shift induced by the presence of a protein corona. This suggests that the concept of protein coronas is likely robust even for more complex objects than nanoparticle monomers. Moreover, the 200 nm PSCOOH NPs form larger clusters than those observed for the smaller PSCOOH NPs (observed at about 500 nm and at higher sizes), confirming the hypothesis of the presence of two complex species: the protein-coated monomer (dimers) and bigger plasma−particle aggregates. The larger size and increased amount of the different species of aggregates with respect to the ones formed by 100 nm PSCOOH NPs prevents the use of DLS to study this system.

As the final example, to illustrate potentially different scenarios for particles with different surfaces, we present data for the hard coronas of sulfonated polystyrene ($PSOSO_3H$, 100 nm, 200 nm) and SiO_2 (50 nm) nanoparticles in Figure 5a−c, respectively. For the bare (100 nm) $PSOSO_3H$ particles in PBS shown in the DCS graph (Figure 5a, empty circles), we do see monomers consistent with the TEM images (see Figure 6a), but in the particle−plasma mixture the particle monomer peak is lost and the intrinsic peak for the pure plasma grows greatly. TEM images of the sulfonated polystyrene 100 nm NP−protein complexes confirm the presence of large clusters involving a larger amount of proteins than was observed for the carboxylated NPs, for which a thin protein layer could be detected, and moreover, monomer complexes were not detected (Figure 6b). The results agree with the picture emerging from the DCS study, but the structural features of the aggregates observed in TEM are not representative of those in solution since both the overnight drying and the gluteraldehyde treatment will affect the complexes' morphology. Interestingly, this indicates that particles partition into the intrinsic protein clusters, rather than associating with or drawing to their surface layers of proteins, illustrating the potential richness of the behavior in biological systems.

Though low in intensity, the monomer peak appears for the 200 nm $PSOSO_3H$ NP−protein complexes (together with peaks for dimers, trimers, etc.) and seems stable with time. Kinetic studies of these "clusters of particles embedded into protein clusters" (see Figure 5a,b) suggest, once more, that the protein−particle complex is extremely long-lived.

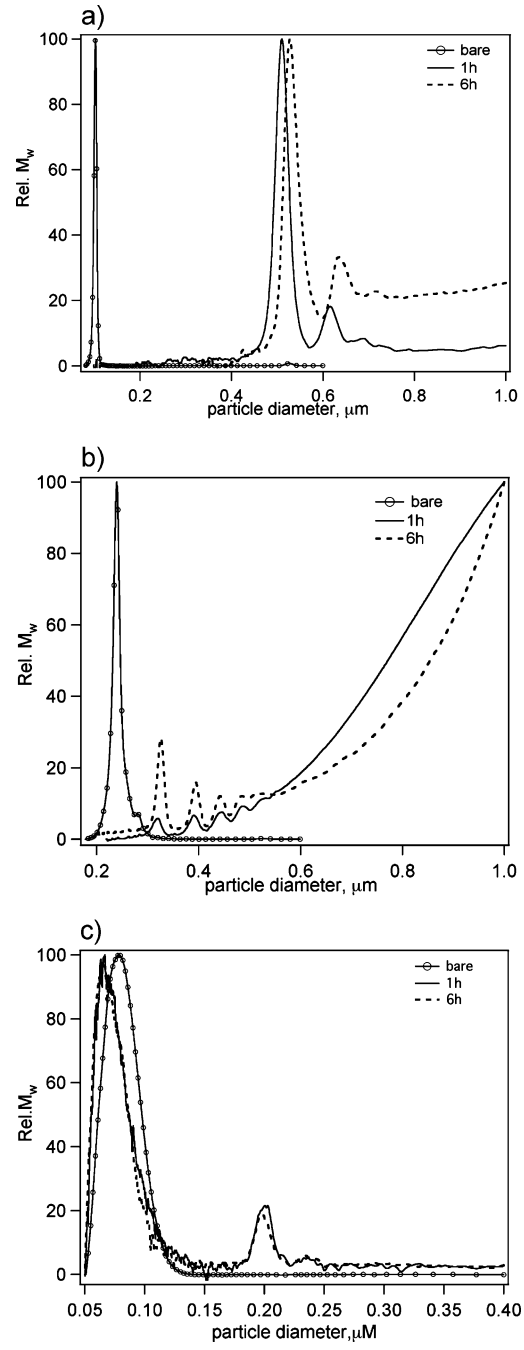

Figure 5. Time-resolved DCS experiments of 100 and 200 nm $PSOSO_3H$ and 50 nm SiO_2 NP−protein complexes. (a) DCS data of 100 nm $PSOSO_3H$ NP−protein complexes free from excess plasma (washed system) as a function of time. (b) DCS data of 200 nm $PSOSO_3H$ NP−protein complexes free from excess plasma (washed system). (c) DCS results for 50 nm SiO_2 NP−protein complexes free from excess plasma (washed system). In all graphs bare NP results (open circles) are reported for reference.

Data for the SiO_2 samples are at first sight surprising since the bare particles appear at a larger "apparent size" than the corona−particle complexes. This artifact is due to the mode of data presentation, using an equivalent uniform density, and is accentuated because the density of silica is significantly different than that of the protein coating. However, a core−shell model (see Methods section in the SI) yields the actual physical structural parameters, namely, a protein shell thickness of about 7 nm as reported in Table S2b in the SI. Hence, DCS experiments of SiO_2 NPs (see Figure 5c) imply largely mono-

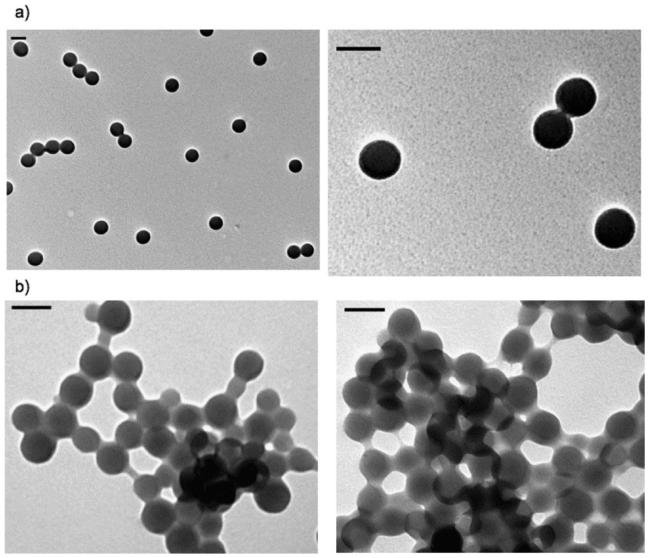

Figure 6. (a) TEM images of bare 100 nm $PSOSO_3H$ NPs fixed in 2.5% gluteraldehyde solution at different magnifications. (b) TEM pictures of 100 nm $PSOSO_3H$ protein−NP complexes free from excess plasma fixed in 2.5% glutaraldehyde solution. Bar = 100 nm.

Table 2. DLS and Zeta-Potential Data of 50 nm SiO_2 NP−Protein Complexes Diluted 500 Times in PBS at 25 °C at $\theta = 173°$[d]

SiO_2 NPs	time [h]	D_H[a] [nm]	PDI[b]	$\langle D_H \rangle$[c] [nm]	z-potential [mV]
washed (1:500)	0	116.6 ± 1.7	0.053	124.9 ± 1.3	−7.0 ± 1.0
washed (1:500)	1	116.3 ± 3.2	0.075	126.7. ± 2.5	−6.0 ± 1.0
washed (1:500)	4	113.0 ± 3.1	0.070	121.4 ± 2.6	−5.8 ± 0.8

[a] z-Average hydrodynamic diameter extracted by cumulant analysis of the data. [b] Polydispersity index from cumulant fitting. [c] Average hydrodynamic diameter determined from CONTIN size distribution. [d] Measurements were made immediately, and 1 and 4 h post-dilution.

meric particles with coronas that behave in much the same manner as for carboxylated polystyrene (PSCOOH), exhibiting the same extraordinary corona stability, as confirmed by the DLS data shown in Table 2. More in-depth studies of SiO_2 and other nanomaterials will appear elsewhere.

Finally, for 100 nm PSCOOH and 50 nm SiO_2 NPs, since the isolated particle−protein complexes (free of excess plasma) are sufficiently stable and their size distribution is dominated by the protein-coated monomeric NPs (small percentage of large aggregates), one can measure their zeta potential (see Tables 1 and 2) and compare these to the bare particles under equivalent PBS conditions (see Table S1a in the SI). Bare particles (in the same medium) have negative zeta potentials of greater magnitude than 30 mV and are therefore strongly charge stabilized. These values are greatly reduced upon formation of the protein corona to the point that, on charge grounds alone, they would not be expected to be colloidal stable. Evidently the corona itself is the origin of the stability.

Discussion and Conclusions

The most striking outcome of this study is that we have been able to obtain a complete structural characterization of NP−protein complexes *in situ* (plasma) and once separated from excess plasma (washed system). Remarkably we see the same protein−particle complexes *in situ* in plasma as in the dispersions isolated by spinning, washing, and resuspending. The high level of stability of those complexes implies that they constitute the primary actors *in situ* in biological dispersions. In our studies, nanoparticles in dispersions typically involve a monomeric nanoparticle core, with a strongly associated and very slowly exchanging protein "hard corona" (consistent with one or two packed protein layers) and particle multimer−corona complexes (dimers, trimers, etc.) present in lower quantities, maintaining their primary structural properties over many hours, sometimes slowly reorganizing into different complexes. There are also more rarely large particle−protein complex assemblies, which for one example (sulfonated polystyrene) actually dominate the dispersion. We note that for flat surfaces many cases arise where proteins and biomolecules in general, once adsorbed on a surface, do not easily leave the surface when the supernatant solution is diluted. The nature and identity of the proteins on the nanoparticles' surface are quite different, and the implications much more far reaching, since nanoparticles can have access to every organ and compartment.[28,29]

The practical implications are that it is possible to study these complexes in isolation, beginning with their layer composition, size, and zeta potential, and studies of protein corona identity, already somewhat advanced, will now become of much higher quality as we learn to work with them in isolation, as well as *in situ*. The fact that particle−hard corona complexes of several materials have low zeta potentials suggests a different dispersion stabilization mechanism from that (such as charge and steric hindrance) typical for bare nanoparticles. Likely their stability is conferred by the specific protein layer characteristics, reminiscent of the design feat by which thousands of different proteins in plasma are colloidal stable despite their crowded environment. Another practical observation is that, although the composition of the different particle−protein organizations in biological media may vary, if well-designed dispersion protocols are used, one can achieve a high level of reproducibility of the populations of different particle−protein organizations (i.e., reproducible amounts of monomer, dimer, trimer, etc., and large complexes). This suggests the possibility of a rational and reproducible approach to studying and understanding bionanoparticle interactions with living organisms in the future.

Moreover, there are implications of these studies for the deeper question of "what living organisms see" in mixtures of nanoparticles and biological fluids. Currently, cellular (uptake, translocation, functional) responses to nanoparticles are presumed to depend on particle size, shape, and material surface presentation, these being currently posed as the basis of systematic studies, predictive approaches (such as quantitative structure−activity relationships), and possibly regulations. The idea that the cell sees the material surface itself must now be re-examined. In some specific cases the cell receptor may have a higher preference for the bare particle surface, but the time scale for corona unbinding illustrated here would still typically be expected to exceed that over which other processes (such as nonspecific uptake) have occurred. Thus, for most cases it is more likely that the biologically relevant unit is not the particle, but a nano-object of specified size, shape, and protein corona structure. The biological consequences of this may not be simple. Naked particle surfaces will have a much greater (nonspecific) affinity for the cell surface than a particle hiding behind a corona of "bystander" proteins, that is, proteins for which no suitable cellular recognition machinery exists. This will strongly affect the physical particle−cell interactions, but may not lead to pronounced biological outcomes. However, constituents of the

(28) Norde, W. *Colloids Surf., B* **2008**, *61*, 1–9.
(29) Shen, H.-H.; Thomas, R. K.; Chen, C.-H.; Darton, R. C.; Baker, S. C.; Penfold, J. *Langmuir* **2009**, *25*, 4211–4218.

long-lived protein corona presenting relevant (cell-facing) binding sites will activate the cellular machinery, if they are in contact with it for long enough. The evidence here suggests that, in comparison to typical cell-membrane-biology event time scales (most occurring over time scales much less than 30 min, many only several minutes in duration), the particle corona is likely to be a defining property of the particle, whether it activates cellular machinery or not. One is driven to the conclusion that, ultimately, it is these long-lived proteins that effectively give the nanoparticle its identity, rather than the particle surface itself. The presence of particle−protein multimers and the larger complexes will be of high significance, and (as a specific example) nanomedicine cannot be expected to advance to application until the immunological consequences of these different coexisting aggregate species are understood for relevant particles. Furthermore, these same issues may be relevant to nanoparticles with surfaces modified by antibodies and proteins, for these particles will in general acquire a new protein corona *in vivo*.

Given the slow exchange of proteins from the hard corona, the short-term interactions of nanoparticles with cells, barriers, and organs may be expected to be dominated by the plasma-derived corona. However, for particles that enter cells, one may also expect modification of the corona in different compartments, and in extreme cases (e.g., following particle localization in lysosomes) one may even expect entire corona removal. *In viv*o the relatively long time that a particle is exposed to a wide variety of biological processing machinery will likely lead to slow exchange of the corona depending on the organ or subsystem involved. Thus, one should not necessarily consider the plasma-derived hard corona as the final long-term corona when the nanoparticle has reached its final location. Indeed, there is some preliminary evidence to suggest that the slowly evolving hard corona may be important in directing the particle to different organs and that once there new coronas derived from biomolecules in those environments arise. Clearly there is a significant amount of work to be done to clarify these issues finally.

Still the overall consequences are clear and far reaching, suggesting that nanoparticle dispersions for biological studies must be treated as a single system in which the choice and origin of serum or plasma (and implicitly, thereby, the test organism), and its preparation, may have a significant bearing on the outcome of experiments. In particular the use of animal (rather than human)-derived media should be reconsidered for some applications.

In summary, some rethinking of the nature of the effective unit in nanobiology, nanomedicine, and nanosafety may be emerging. In turn, this suggests the need for revised thinking on useful physiochemical (and other) methods of characterization of biologically relevant nanomaterials, to account for their actual composition *in situ* in complex biological milieu.

Acknowledgment. This work was conducted under the framework of the INSPIRE Programme, funded by the Irish Government's Programme for Research in Third Level Institutions, Cycle 4, National Development Plan 2007−2013. The work is also based on work performed within the SFI SRC BioNanoInteract (07 SRC B1155). Additional financial support from FP6 IST project SIGHT (IST-2005-033700) and EU FP6 project NanoInteract (NMP4-CT-2006-033231) is acknowledged. We thank the Electron Microscopy Laboratory of the Conway Institute for Biomolecular and Biomedical Research in UCD and Dr. David Cottell for his help with the TEM experiments. Paulo Pinto is acknowledged for fruitful discussions regarding the DCS data analysis.

Supporting Information Available: Experimental Section. A detailed description of the core−shell method used to analyze the DCS data, a basic physicochemical characterization of the nanoparticle dispersions in PBS. Results. DCS data for pure plasma and nanoparticle dispersions in PBS, additional TEM and DCS results of 100 nm NP−protein complexes under different conditions with gel studies on the composition of the protein corona, and a complete analogue study for 200 nm PSCOOH NP−protein complexes. This material is available free of charge via the Internet at http://pubs.acs.org.

JA910675V